

**STEREOCHEMICAL INFLUENCE OF THE
 PENTAMETHYLCYCLOPENTADIENYL LIGAND ON
 THE ISOCYANIDE INSERTION REACTIONS OF THE
 1-SILA-3-HAFNACYCLOBUTANE COMPLEX,
 (C₅Me₅)(C₅H₅)Hf(CH₂SiMe₂CH₂)***

LIOBA KLOPPENBURG¹ and JEFFREY L. PETERSEN†

Department of Chemistry, West Virginia University, Morgantown, WV 26506-6045, U.S.A.

Abstract—The insertion reactions of CNMe and CN-*t*-Bu with Cp*₂Hf(CH₂SiMe₂CH₂), **1**, have been investigated to evaluate the stereoelectronic influence of the Cp* ligand on the competitive 1,2-silyl shift and reductive coupling pathways previously observed for Cp₂Hf(CH₂SiMe₂CH₂). Under ambient conditions the addition of CNMe to **1** proceeds with the sequential formation of Cp*₂Hf(N(Me)C(=CH₂)SiMe₂CH₂), **2**, and Cp*₂Hf(N(Me)C(=CH₂)SiMe₂(CH₂=)CN(Me)), **3**. Alternatively, the addition of excess CNMe below –5°C to **1** occurs with reductive coupling to produce Cp*₂Hf(N(Me)C(CH₂SiMe₂CH₂)=CN(Me)), **4**. In contrast, the addition of two equivalents of CN-*t*-Bu to **1** does not afford the corresponding cyclic enamide species but proceeds with the sequential formation of Cp*₂Hf(N(CMe₃)CCH₂SiMe₂CH₂), **5**, and Cp*₂Hf(N(CMe₃)C–C(=NCMe₃)CH₂SiMe₂CH₂), **6**. The molecular structures of **3** and **6** have been determined by X-ray crystallography. The puckered 1-sila-3,5-diaza-4-hafnacyclohexane ring of **3** adopts a chair conformation with the folding along the N···N' vector being 19.3° out of the N', Hf, N plane toward the smaller Cp ligand and the folding along the C(1)···C(1)' vector being 43.3° in the opposite direction toward the Cp* ligand. The molecular structure of **6** is consistent with nucleophilic attack of CN-*t*-Bu at the η²-iminoacyl carbon of **5** occurring exclusively from the side opposite to the Cp* ligand. The second equivalent of CN-*t*-Bu displaces the η²-iminoacyl group away from the Hf atom, eventually placing the resultant imine group of **6** *syn* to the Cp* ligand.

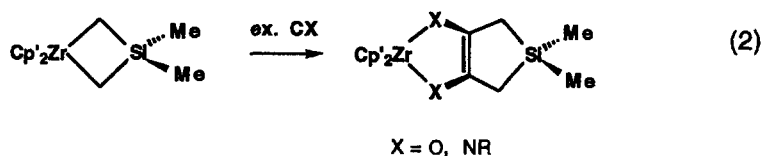
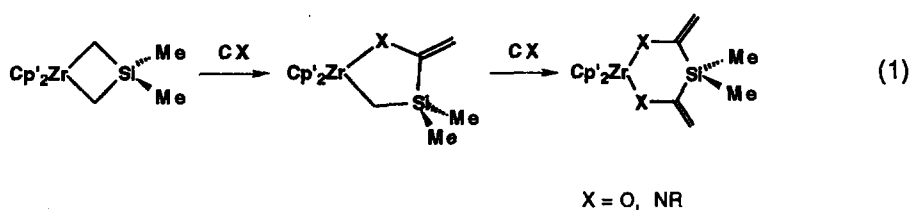
Our investigations of the CO² and isocyanide³ insertion chemistry of electrophilic 1-sila-3-zirconacyclobutane complexes, such as Cp'₂Zr(CH₂SiMe₂CH₂) [Cp' = Cp(C₅H₅) or Cp*(C₅Me₅)] have led to the observation of two competitive reaction pathways, one involving two consecutive intramolecular 1,2-silyl shifts⁴ to produce the respective cyclic dienolate and dienamide compounds

(eq. 1) and the other proceeding with reductive coupling⁵ to afford the isomeric bicyclic enediolate and enediamidate complexes, respectively (eq. 2). Direct evidence for the dicyclic η²-iminoacyl species, Cp'₂M(N(R)CCH₂SiMe₂CH₂), as the common intermediate in the 1,2-silyl shift and reductive coupling reactions of CNR was provided during our subsequent study of the reaction of CN-*t*-Bu with Cp₂Hf(CH₂SiMe₂CH₂).⁶

In the course of our investigations it became apparent that the steric size of the cyclopentadienyl ligand and/or the alkyl substituent of the isocyanide could significantly influence the course of these

* On the occasion of the 50th birthday of Professor John E. Bercaw, a good friend and colleague.

† Author to whom correspondence should be addressed.



insertion reactions. Specifically, whereas the addition of two equivalents of CN-*t*-Bu to $\text{Cp}_2\text{M}(\text{CH}_2\text{SiMe}_2\text{CH}_2)$ ($\text{M} = \text{Zr},^{3a} \text{Hf}^6$) proceeds with the formation of $\text{Cp}_2\text{M}(\text{N}(\text{CMe}_3)\text{C}=\text{NCMe}_3)\text{CH}_2\text{SiMe}_2\text{CH}_2$ which in turn rearranges intramolecularly upon heating to the bicyclic enediamidate species, the corresponding isocyanide reductive coupling reaction for $\text{Cp}_2\text{Zr}(\text{CH}_2\text{SiMe}_2\text{CH}_2)^{3a,c}$ occurs for CNMe but not for CN-*t*-Bu. This difference in reactivity is likely due to the ability of the larger Cp* ligands of $\text{Cp}_2\text{Zr}(\text{CH}_2\text{SiMe}_2\text{CH}_2)$ to either block the CN-*t*-Bu from attacking the electrophilic carbon of the η^2 -iminoacyl intermediate or prohibit the formation of the η^2 -iminoacyl intermediate.

The outcome of MO calculations performed on $\text{Cp}_2\text{Zr}(\text{N}(\text{CMe}_3)\text{CCH}_2\text{SiMe}_2\text{CH}_2)^7$ revealed that the LUMO is symmetrically disposed with respect to the three-membered ZrCN ring.^{8,9} This feature implies that the second equivalent of CN-*t*-Bu can attack the electrophilic η^2 -iminoacyl carbon of $\text{Cp}_2\text{Zr}(\text{N}(\text{CMe}_3)\text{CCH}_2\text{SiMe}_2\text{CH}_2)$ from either face of the ZrCN ring with equal probability. Therefore, one might anticipate that the replacement of one of the two Cp ligands of $\text{Cp}_2\text{M}(\text{CH}_2\text{SiMe}_2\text{CH}_2)$ with the Cp* ligand will sterically differentiate these two faces of the corresponding η^2 -iminoacyl species and thereby provide an opportunity to evaluate directly the stereochemical influence of the Cp* ligand on the course of the isocyanide reductive coupling reaction. To test this hypothesis, we prepared the mixed-cyclopentadienyl ring 1-sila-3-hafnacyclobutane complex, $\text{Cp}^*\text{CpHf}(\text{CH}_2\text{SiMe}_2\text{CH}_2)$, **1**, and examined its reactivity with both CNMe and CN-*t*-Bu. The results of these experiments and our structural analyses of $\text{Cp}^*\text{CpHf}(\text{N}(\text{Me})\text{C}(\text{=CH}_2)\text{SiMe}_2$

$(\text{CH}_2\text{=})\text{CN}(\text{Me}))$, **3**, and $\text{Cp}^*\text{CpHf}(\text{N}(\text{CMe}_3)\text{C}=\text{C}(\text{=NCMe}_3)\text{CH}_2\text{SiMe}_2\text{CH}_2)$, **6**, are described herein and provide further chemical information regarding the course of the C,C-coupling reaction.

EXPERIMENTAL

Reagents

All solvents were purified by standard procedures and vacuum distilled into storage flasks containing either $[\text{Cp}_2\text{Ti}(\mu\text{-Cl})_2]_2\text{Zn}^{10}$ (hydrocarbon and ethereal solvents) or P_4O_{10} (chlorinated solvents). Hexamethyldisiloxane was distilled from LiAlH_4 . Benzene-*d*₆ and toluene-*d*₈ (Cambridge Isotope Laboratories) were vacuum distilled from 4A molecular sieves. *tert*-Butyl isocyanide (Aldrich) was dried over activated molecular sieves and distilled before use. Methyl isocyanide,¹¹ $\text{C}_3\text{Me}_5\text{H}$,¹² $[\text{MgCH}_2\text{SiMe}_2\text{CH}_2]_m$,¹³ Cp^*HfCl_3 ,¹⁴ and $\text{Cp}^*\text{CpHfCl}_2$ ¹⁵ were prepared by literature procedures.

General considerations

All manipulations and reactions were carried out on a double-manifold, high-vacuum line or in a Vacuum Atmospheres glovebox equipped with a HE-493 Dri-Train. Nitrogen was purified by passage over reduced BTS catalyst and activated 4A molecular sieves. All glassware was thoroughly oven-dried and flame dried under vacuum. NMR sample tubes were sealed under approximately 500 Torr of nitrogen. The addition of a stoichiometric quantity of a volatile isocyanide to a reaction solution was accomplished with a calibrated gas bulb. The instrumentation employed for the measure-

ment of the 1H and ^{13}C NMR spectra of the hafnium compounds has been described previously.⁶ Elemental analyses were carried out by Robertson Microlit Laboratories, Inc. of Madison, NJ.

Preparation of $Cp^*CpHf(CH_2SiMe_2CH_2)$, **1**

$Cp^*CpHfCl_2$ (1.30 g, 3.10 mmol) and $[Mg(CH_2SiMe_2CH_2)]_n$ (0.69 g, 6.23 mmol) were suspended in 30 cm³ of toluene. The reaction mixture was stirred and refluxed at 110°C for 5 days. After removal of solvent, the product residue was extracted twice with 50 cm³ of pentane and the soluble product was dried *in vacuo*. Sublimation at 60°C and 10⁻⁴ Torr gave 0.97 g (67% yield) of **1** as white crystals. 1H NMR spectrum in benzene-*d*₆ (mult., $^2J_{H-H}$ in Hz): δ 5.63 (C_5H_5 , s), 1.74 (CCH_3 , s), 1.36, 0.60 ($HfCH_2$, dd, 13.5), 0.40, 0.35 ($SiMe_2$, s); gated non-decoupled ^{13}C NMR spectrum (mult., $^1J_{C-H}$ in Hz): δ 115.8 (CCH_3 , s), 109.8 (C_5H_5 , d, 172.1), 48.3 ($HfCH_2$, t, 123), 11.9 (CCH_3 , q, 126), 2.8, -1.9 ($SiMe_2$, q, 118, 120). Found: C, 48.81; H, 6.46; N, 0.0. Calc. for $C_{19}H_{30}HfSi$: (465.02) C, 49.08; H, 6.50; N, 0.0.

Preparation of $Cp^*CpHf(N(Me)C(=CH_2)SiMe_2(CH_2)CN(Me))$, **3**

A 0.25 g sample of **1** was placed in a 100 cm³ solv-seal flask attached to a calibrated gas bulb. The compound was dissolved in 25 cm³ of pentane and 1 equivalent of CNMe was admitted in small increments over a period of several days. After stirring the reaction mixture for an additional week at room temperature, the solvent was removed leaving a yellow residue. NMR measurements confirmed the complete conversion of **1** to the cyclic enamide, $Cp^*CpHf(N(Me)C(=CH_2)SiMe_2CH_2)$, **2**. After redissolving **2** in pentane, a second equivalent of CNMe was introduced and the resultant solution was stirred for an additional 2 days. Removal of the solvent left a yellow residue, which was washed three times with 20 cm³ of hexamethyldisiloxane. Recrystallization from pentane yielded suitable crystals of **3** for an X-ray structural analysis. 1H NMR spectrum of **2** in benzene-*d*₆ (mult., $^2J_{H-H}$ in Hz): δ 5.83 (C_5H_5 , s), 4.27, 4.19 ($=CH_2$, s), 2.16 (NCH_3 , s), 1.74 (C_5Me_5 , s), 1.10, 0.93 ($HfCH_2$, dd, 12.6), 0.51, 0.40 ($SiMe_2$, s); gated nondecoupled ^{13}C NMR spectrum of **2** (mult., $^1J_{C-H}$ in Hz): δ 161.5 ($C=CH_2$, s), 118.5 (CCH_3 , s), 111.1 (C_5H_5 , d, 172), 86.1 ($=CH_2$, dd, 151, 156), 41.8 ($HfCH_2$, 117), 35.1 ($NCMe_3$, q, 132), 11.6 (CCH_3 , q, 126), 3.03, 2.56 ($SiMe_2$, q, 119, 119). 1H NMR spectrum of **3** in benzene-*d*₆ (mult., $^2J_{H-H}$ in Hz): δ 5.91

(C_5H_5 , s), 4.60, 4.54 ($=CH_2$, s), 2.30 (NCH_3 , s), 1.77 (C_5Me_5 , s), 0.54, 0.52 ($SiMe_2$, s); gated non-decoupled ^{13}C NMR spectrum of **3** (mult., $^1J_{C-H}$ in Hz): δ 161.4 ($C=CH_2$, s), 121.1 (CCH_3 , s), 111.7 (C_5H_5 , d, 171), 93.3 ($=CH_2$, d, 153, 155), 36.1 ($NCMe_3$, q, 133), 11.9 (CCH_3 , q, 127), 1.05 ($SiMe_2$, q, 120). Found: C, 50.08; H, 6.86; N, 4.89. Calc. for $C_{23}H_{36}HfSiN_2$ (547.13): C, 50.46; H, 6.63; N, 5.12.

Preparation of $Cp^*CpHf(N(Me)C(CH_2SiMe_2CH_2)=CN(Me))$, **4**

The reaction of **1** with excess CNMe was performed on a small scale to confirm that this compound can reductively couple CNMe. A 0.052 g sample of $Cp^*CpHf(CH_2SiMe_2CH_2)$ was dissolved in 10 cm³ of pentane and 4 equivalents of CNMe were added from a calibrated gas bulb via vacuum transfer to the reaction vessel. The reaction mixture was stirred at -30°C overnight and then slowly warmed over a period of several hours to -5°C. The orange-brown solution was stirred for one more day and then evaporated to dryness. A 1H NMR spectrum of the oily reddish brown residue indicated the presence of one predominant species, **4**. 1H NMR spectrum of **4** in benzene-*d*₆ (mult., $^2J_{H-H}$ in Hz): δ 5.45 (C_5H_5 , s), 3.34 (NCH_3 , s), 1.88 (CCH_3 , s), 1.89, 1.44 ($=CCH_2$, dd, 16.7), 0.18, 0.14 ($SiMe_2$, s); gated non-decoupled ^{13}C NMR spectrum (mult., $^1J_{C-H}$ in Hz): δ 137.4 (NC , s), 114.9 (CCH_3 , s), 102.8 (C_5H_5 , d, 170), 40.8 (NCH_3 , q, 133), 16.7 ($=CCH_2$, t, 123), 11.6 (CCH_3 , q, 126), -0.39, -0.96 ($SiMe_2$, q, 118, 118).

Reaction of tert-Butyl isocyanide with $Cp^*CpHf(CH_2SiMe_2CH_2)$

This reaction was performed initially on an NMR scale. Two equivalents of CN-*t*-Bu were added to a C_6D_6 solution of **1** (0.031 g, 0.066 mmol). Periodic 1H NMR measurements indicated that the reaction proceeds with the rapid insertion of 1 equivalent of CN-*t*-Bu to give $Cp^*CpHf(N(CMe_3)CCH_2SiMe_2CH_2)$, **5**. This species slowly takes up another equivalent of CN-*t*-Bu to give a single product, the η^2 -iminoacyl imine complex, $Cp^*CpHf(N(CMe_3)C-C(=NCMe_3)CH_2SiMe_2CH_2)$, **6**. This double insertion reaction was then performed on a larger scale reaction to isolate **6** for further characterization. A 30 cm³ pentane solution of **1** (0.80 g, 1.72 mmol) was charged with 0.50 cm³ (4.43 mmol) of CN-*t*-Bu. The yellow reaction mixture was stirred at room temperature for 6

days. Removal of the solvent yielded a foamy residue which was washed twice with 20 cm³ of hexamethyldisiloxane. A light yellow powder was obtained. Recrystallization by slow diffusion of the pentane solvent into hexamethyldisiloxane produced suitable single crystals of **6** for an X-ray crystallographic analysis. ¹H NMR spectrum of **5** in benzene-*d*₆ (mult., ²*J*_{H-H} in Hz): δ 5.66 (C₅H₅, s), 2.79, 2.47 (CCH₂Si, dd, 12.6), 1.73 (CH₃, s), 1.20 (NCMe₃, s), 0.53, 0.02 (SiMe₂, s), -0.31, -0.46 (HfCH₂, dd, 12.3); gated non-decoupled ¹³C NMR spectrum of **5** (mult., ¹*J*_{C-H} in Hz): δ 242.9 (HfCN, s), 112.9 (CCH₃, s), 107.4 (C₅H₅, d, 170), 58.1 (NCMe₃, s), 33.4 (CCH₂Si, t, 113), 30.6 (NCMe₃, q, 126), 16.7 (HfCH₂Si, dd, 118), 12.1 (CCH₃, q, 126), 4.89, 0.55 (SiMe₂, q, 117, 118). ¹H NMR spectrum of **6** in benzene-*d*₆ (mult., ²*J*_{H-H} in Hz): δ 5.67 (C₅H₅, s), 2.23, 1.10 (CCH₂Si, dd, 13.2), 1.79 (CCH₃, s), 1.42, 1.32 (NCMe₃, s), 0.43, 0.35 (SiMe₂, s), -0.15, -1.15 (HfCH₂, dd, 11.6); gated non-decoupled ¹³C NMR spectrum of **6** (mult., ¹*J*_{C-H} in Hz): δ 239.3 (HfCN, s), 170.8 (C=NCMe₃, s), 114.0 (CCH₃, s), 107.4 (C₅H₅, d, 171), 62.1, 55.4 (NCMe₃, s), 31.7 (NCMe₃, q, 126), 30.7 (CH₂Si, t, 112), 14.8 (HfCH₂Si, t, 109), 12.0 (CCH₃, q, 126), 8.27, 3.51 (SiMe₂, q, 122, 117). Found: C, 54.95; H, 7.62; N, 4.34. Calc. for C₂₉H₄₈HfSiN₂ (631.26): C, 55.18; H, 7.66; N, 4.44.

X-Ray structural analyses of **3** and **6**

The X-ray structural analyses of **3** and **6** were performed by following the same general procedures. A single crystal of each compound was sealed in a capillary tube under a nitrogen atmosphere and then optically aligned on the goniostat of a Siemens P4 automated X-ray diffractometer. The corresponding lattice parameters and orientation matrix for the respective orthorhombic unit cell were determined from a least-squares fit of the orientation angles of at least 20 higher order reflections at 22°C. The systematic absences observed for **3** of $\{hkl\}$, $h+k=2n+1$, $\{h0l\}$, $l=2n+1$ are consistent with the non-centrosymmetric space group *Cmc*2₁ (*C*_{2v}, No. 36) and the centrosymmetric space group *Cmcm* (*D*_{2h}, No. 63), whereas the systematic absences observed for **6** of $\{0kl\}$, $k+l=2n+1$, $\{h0l\}$, $h=2n+1$ are consistent with the non-centrosymmetric space group *Pna*2₁ (*C*_{2v}, No. 33) and the centrosymmetric space group *Pnam* (*D*_{2h}, No. 62). In each case, the non-centrosymmetric space group was confirmed as the correct one by the results of the structural analysis. The refined lattice parameters and other pertinent

crystallographic information are summarized in Table 1.

Intensity data were measured at 22±1°C with graphite-monochromated Mo-*K*_α radiation (λ = 0.71073 Å) and ω scans with variable scan rates (2–5° min⁻¹). Background counts were measured at the beginning and at the end of each scan with the crystal and counter kept stationary. The intensities of three standard reflections were measured after every 100 reflections during data collection and showed no evidence of crystal movement. The intensity data were corrected for Lorentz-polarization, absorption and any crystal decay.

The structure solution for **3** was initiated by the heavy-atom method. The fractional coordinates of the Hf atom, which lies on a crystallographically-imposed mirror plane, were determined by an interpretation of the Harker vectors obtained from the corresponding Patterson map calculated with SHELXTL PC operating on a St. Clair 486 Clairstation. The approximate coordinates of the independent non-hydrogen atoms were revealed by Fourier methods and the hydrogen atom positions were idealized with isotropic temperature factors set at 1.2 times that of the adjacent carbon. The methyl protons of C9 are disordered in a staggered arrangement about a crystallographic mirror plane whereas the methyl protons of C3 and C4 are not. Full-matrix least-squares refinement, based upon the minimization of $\sum w_i |F_o^2 - F_c^2|^2$, with $w_i^{-1} = [\sigma^2(F_o^2) + (0.0409 P)^2 + 0.24 P]$ where $P = [\text{Max}(F_o^2, 0) + 2F_o^2]/3$, was performed with SHELXL-93¹⁶ operating on a Professional Computer Systems 486 66MHz PC and converged to give final discrepancy indices¹⁷ for the 17 unique non-hydrogen atoms and the 21 unique hydrogen atoms of $R_1 = 0.0299$, $wR_2 = 0.0689$ and GOF = 1.042 for 2491 reflections with $I > 2\sigma(I)$. A selected listing of the interatomic distances and bond angles for **3** is provided in Table 2.

In contrast, initial fractional coordinates for the Hf and Si atoms in **6** were determined by direct methods with SHELXTL IRIS. The approximate coordinates of the remaining non-hydrogen atoms were revealed by subsequent Fourier calculations and the hydrogen atom positions were idealized with isotropic temperature factors set at 1.2 times that of the adjacent carbon. Full-matrix least-squares refinement, based upon the minimization of $\sum w_i |F_o^2 - F_c^2|^2$ with $w_i^{-1} = [\sigma^2(F_o^2) + (0.0246 P)^2]$ where $P = [\text{Max}(F_o^2, 0) + 2F_o^2]/3$, was performed with SHELXL-93¹⁶ operating on a Silicon Graphics Iris Indigo workstation and converged to give final discrepancy indices¹⁷ for the 33 non-hydrogen atoms and the 48 hydrogen atoms of $R_1 = 0.0466$,

Table 1. Crystallographic data for the X-ray diffraction analyses of **3** and **6**

| | | |
|----------------------------------|-----------------------------------|-----------------------------------|
| Emp. formula | $C_{23}H_{36}HfN_2Si$, 3 | $C_{29}H_{48}HfN_2Si$, 6 |
| Color | red–orange | pale yellow |
| Cryst. dimensions (mm) | $0.35 \times 0.375 \times 0.19$ | $0.10 \times 0.20 \times 0.40$ |
| Crystal system | orthorhombic | orthorhombic |
| Space group | $Cmc2_1$ | $Pna2_1$ |
| a (Å) | 14.033(4) | 17.948(2) |
| b (Å) | 10.684(3) | 10.724(1) |
| c (Å) | 15.823(4) | 15.694(2) |
| V (Å ³) | 2372.3(11) | 3020.7(6) |
| Z | 4 | 4 |
| Formula weight (amu) | 547.12 | 631.27 |
| Density (g cm ⁻³) | 1.532 | 1.388 |
| μ (cm ⁻¹) | 44.57 | 35.11 |
| $F(000)$ | 1096 | 1288 |
| 2θ range (°) | 4.80–55.00 | 4.40–55.00 |
| No. of data collected | 3384 | 4536 |
| No. of unique data | 2829 ($R_{int} = 0.0297$) | 3849 ($R_{int} = 0.0314$) |
| Data with $I > 2\sigma(I)$ | 2491 | 2500 |
| Absorption correction | empirical (PSI scans) | empirical (PSI scans) |
| R indices ($I > 2\sigma(I)$) | $R_1 = 0.0299$ $wR_2 = 0.0689$ | $R_1 = 0.0466$ $wR_2 = 0.0668$ |
| R indices (all data) | $R_1 = 0.0397$ $wR_2 = 0.0725$ | $R_1 = 0.0983$ $wR_2 = 0.0806$ |
| σ_1 , GOF | 1.042 | 1.000 |
| No. of variables | 135 | 311 |
| Data to parameter ratio | 20.3 : 1 | 12.5 : 1 |
| Largest difference peak and hole | 1.334, –0.535 | 1.166, –0.609 |

Table 2. Interatomic distances (Å) and bond angles (°) for **3'**

| Interatomic distances | | | |
|---|-----------|-----------------|-----------|
| Hf—N | 2.103(6) | Hf—Cp*(c) | 2.274 |
| Hf—Cp(c) | 2.231 | N—C(5) | 1.496(11) |
| N—C(1) | 1.394(11) | Si—C(1) | 1.861(12) |
| C(1)—C(2) | 1.377(14) | Si—C(4) | 1.88(2) |
| Si—C(3) | 1.78(2) | | |
| range of Hf—C(Cp) distances: 2.492(8)–2.562(12) | | | |
| range of Hf—C(Cp*) distances: 2.553(13)–2.580(10) | | | |
| Bond angles | | | |
| N'—Hf—N | 97.5(4) | Cp(c)—Hf—Cp*(c) | 129.3 |
| C(1)—Si—C(1)' | 110.0(5) | C(1)—Si—C(3) | 108.6(5) |
| C(1)—Si—C(4) | 111.5(4) | C(3)—Si—C(4) | 106.5(10) |
| C(1)—N—Hf | 124.8(6) | N—C(1)—Si | 116.8(6) |
| C(5)—N—Hf | 116.2(6) | N—C(1)—C(2) | 121.9(12) |
| C(1)—N—C(5) | 113.4(9) | Si—C(1)—C(2) | 121.1(10) |

^aCp(c) and Cp*(c) are the centroids of the cyclopentadienyl ring and the pentamethylcyclopentadienyl ring, respectively. Cp(c) contains carbon atoms C(6), C(7), C(8), C(7)' and C(8)' and Cp*(c) was calculated from the atomic coordinates of carbon atoms C(9), C(10), C(11), C(10)' and C(11)'. The prime (') notation refers to the corresponding symmetry-related atom.

$wR_2 = 0.0668$ and $GOF = 1.000$ for 2500 reflections with $I > 2\sigma(I)$. A selected listing of interatomic distances and bond angles for **6** are given in Table 3.

RESULTS AND DISCUSSION

The metathetical reaction of $\text{Cp}^*\text{CpHfCl}_2$ and $[\text{Mg}(\text{CH}_2\text{SiMe}_2\text{CH}_2)]_n$ in refluxing toluene provides a convenient method for the preparation of $\text{Cp}^*\text{CpHf}(\text{CH}_2\text{SiMe}_2\text{CH}_2)$, **1**. This 1-sila-3-hafnacyclobutane complex is easily purified by sublimation and was characterized by ^1H and ^{13}C NMR measurements and elemental analysis. Its ^1H NMR and ^{13}C NMR spectra each exhibit six characteristic resonances that are readily assigned. The protons of the methylene groups are diastereotopic and therefore appear as an AB-quartet centered at δ 1.36 and 0.60 with $^2J_{\text{H-H}} = 13.5$ Hz. The two magnetically inequivalent methyl groups bound to silicon exhibit separate singlets at δ 0.40 and 0.35. In the corresponding gated non-decoupled ^{13}C NMR spectrum the methylene carbon resonance of **1** appears as a "pseudo-triplet" at δ 48.3 with $^1J_{\text{C-H}} = 123$ Hz, indicating that $^1J_{\text{C-Ha}} \approx ^1J_{\text{C-Hb}}$. The two methyl carbons bound to silicon appear as two sep-

arate quartets at δ 2.8 and -1.9 with $^1J_{\text{C-H}} = 118$ and 120 Hz, respectively.

The migratory insertion reactions of methyl isocyanide and *tert*-Butyl isocyanide with **1** were performed to evaluate the stereoelectronic influence of the Cp^* ligand on the course of the insertion chemistry. Each reaction product was identified by solution NMR measurements and when possible the molecular structure was verified by X-ray crystallography.

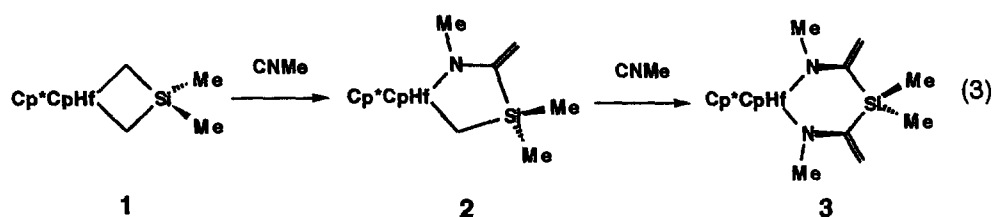
Methyl isocyanide insertion chemistry of $\text{Cp}^\text{CpHf}(\text{CH}_2\text{SiMe}_2\text{CH}_2)$*

The addition of CNMe to **1** proceeds at ambient temperature with the insertion of CNMe into both Hf—C bonds of the 1-sila-3-hafnacyclobutane ring and with the sequential formation of the cyclic enamide, $\text{Cp}^*\text{CpHf}(\text{N}(\text{Me})\text{C}(=\text{CH}_2)\text{SiMe}_2\text{CH}_2)$, **2**, and the cyclic dienamide complex, $\text{Cp}^*\text{CpHf}(\text{N}(\text{Me})\text{C}(=\text{CH}_2)\text{SiMe}_2(\text{CH}_2=\text{CN}(\text{Me})))$, **3** (eq. 3). Each Hf-induced CNMe insertion is followed by an intramolecular 1,2-silyl shift. The solution ^1H and ^{13}C NMR spectra of **2** and **3** reflect the symmetry at each Hf center.

Table 3. Interatomic distances (Å) and bond angles (°) for **6**^a

| Interatomic distances | | | |
|---|-----------|-----------------|-----------|
| Hf—C(1) | 2.201(12) | Hf—N(1) | 2.242(8) |
| Hf—C(4) | 2.28(2) | Hf—Cp*(c) | 2.255 |
| Hf—Cp(c) | 2.252 | Si—C(4) | 1.87(2) |
| Si—C(3) | 1.92(2) | Si—C(6) | 1.888(14) |
| Si—C(5) | 1.876(13) | N(2)—C(2) | 1.262(14) |
| N(1)—C(1) | 1.26(2) | N(2)—C(11) | 1.458(14) |
| N(1)—C(7) | 1.526(13) | C(2)—C(3) | 1.51(2) |
| C(1)—C(2) | 1.47(2) | | |
| range of Hf—C(Cp) distances: 2.514(12)–2.558(13) | | | |
| range of Hf—C(Cp*) distances: 2.514(11)–2.581(12) | | | |
| Bond angles | | | |
| C(1)—Hf—N(1) | 32.9(4) | C(1)—Hf—C(4) | 77.8(5) |
| N(1)—Hf—C(4) | 109.8(6) | Cp(c)—Hf—Cp*(c) | 130.5 |
| C(3)—Si—C(4) | 109.5(7) | C(3)—Si—C(5) | 104.6(7) |
| C(3)—Si—C(6) | 109.4(6) | C(4)—Si—C(5) | 117.4(7) |
| C(4)—Si—C(6) | 110.6(7) | C(5)—Si—C(6) | 105.0(7) |
| Hf—N(1)—C(1) | 71.8(7) | Hf—C(1)—N(1) | 75.3(7) |
| Hf—N(1)—C(7) | 157.3(7) | Hf—C(1)—C(2) | 147.6(9) |
| C(1)—N(1)—C(7) | 129(2) | N(1)—C(2)—C(3) | 135.9(13) |
| C(1)—C(2)—N(2) | 118.1(12) | C(1)—C(2)—C(3) | 107.6(11) |
| N(2)—C(2)—C(3) | 133.7(13) | C(2)—N(2)—C(11) | 126.3(11) |
| C(2)—C(3)—Si | 116.1(10) | Hf—C(4)—Si | 123.9(8) |

^a Cp(c) and Cp*(c) are the centroids of the cyclopentadienyl ring and the pentamethylcyclopentadienyl ring, respectively. Cp(c) contains atoms C(15) through C(19) and Cp*(c) was calculated from the atomic coordinates of C(20) through C(24).



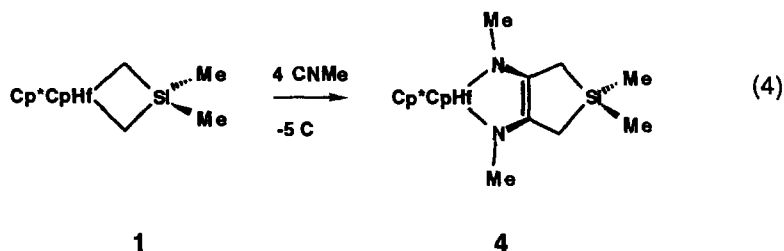
In both complexes the methyl substituents of the $SiMe_2$ group are chemically inequivalent. The protons of the Hf-bound methylene of **2** are diastereotopic and appear as a second-order AB-quartet at δ 1.10 and 0.93 with $^2J_{H-H} = 12.6$ Hz. The magnetically inequivalent protons of the exocyclic methylene of **2** exhibit a pair of singlets at δ 4.27 and 4.19, with the corresponding methylene carbon resonance observed at δ 86.1 as a doublet of doublets with $^1J_{C-H} = 151$ and 156 Hz. The corresponding magnetically inequivalent protons of the two chemically-equivalent exocyclic methylenes of **3** exhibit a characteristic pair of singlets at δ 4.60 and 4.54, with the methylene carbon resonance appearing as a doublet of doublets centered at δ 93.3 with $^1J_{C-H} = 153$ and 155 Hz. The quaternary carbons attached to the Si and N atoms of the five and six-membered hafnacyclic rings of **2** and **3** are resolved as a low intensity singlet at δ 161.5 and 161.4, respectively. The remaining NMR resonances are observed in their expected locations.

The reaction of excess CNMe with **1** below $-5^\circ C$ proceeds with the reductive coupling of two equivalents of CNMe to give the bicyclic enediamidate complex, $Cp^*CpHf(N(Me)C(=CH_2)SiMe_2)C(=CH_2)CN(Me)$, **4** (eq. 4). Its identity was confirmed

resonance centered at δ 16.7 has $^1J_{C-H} = 123$ Hz, consistent with sp^3 hybridization. The methyl protons of the $SiMe_2$ group exhibit two separate singlets at δ 0.14 and 0.18, whereas the carbon resonances for these methyl groups appear as two distinct quartets at δ -0.39 and -0.96 with $^1J_{C-H} = 118$ Hz. The methyl proton and carbon resonances of the coupled CNMe groups are observed as a singlet at δ 3.34 and as a quartet at δ 40.8 with $^1J_{C-H} = 133$, respectively. The low intensity singlet at δ 137.4 is tentatively assigned to the double-bonded quaternary carbons of the bicyclic enediamido ligand. The remaining resonances for the cyclopentadienyl ligands are readily assigned.

Description of the molecular structure of
 $Cp^*CpHf(N(Me)C(=CH_2)SiMe_2)$
 $(CH_2=)CN(Me)$

A perspective view of the molecular structure of this cyclic dienamide is depicted in Fig. 1 with the non-hydrogen atom numbering scheme. The molecular geometry is constrained by a crystallographic mirror plane that passes through the Hf, Si, C(3), C(4), C(6), C(9), and C(12) atoms. The coor-



by NMR measurements. The chemical shifts and the $^2J_{H-H}$ and $^1J_{C-H}$ coupling constants are comparable to those reported for $Cp_2^*Zr(N(Me)C(=CH_2)SiMe_2)C(=CH_2)CN(Me)$.^{3c} As expected, the protons of the symmetry-related methylene groups are diastereotopic and the methyl substituents of the $SiMe_2$ group are chemically inequivalent. The two methylene protons appear as an AB-quartet at δ 1.89 and 1.44 with $^2J_{H-H} = 16.7$ Hz; the pseudo-triplet for the methylene carbon

dination environment of the hafnium atom consists of canted η^5 -pentamethylcyclopentadienyl and η^5 -cyclopentadienyl ligands which are arranged in a staggered orientation and the two N donor atoms of the 1-sila-3,5-diaza-4-hafnacyclohexane ring, which contains two exocyclic methylene groups. The N', Hf, N plane is disposed asymmetrically with respect to the planar internal carbon rings of the Cp^* and Cp ligands, as evidenced by the respective acute dihedral angles of 28.5° and 24.1° . The

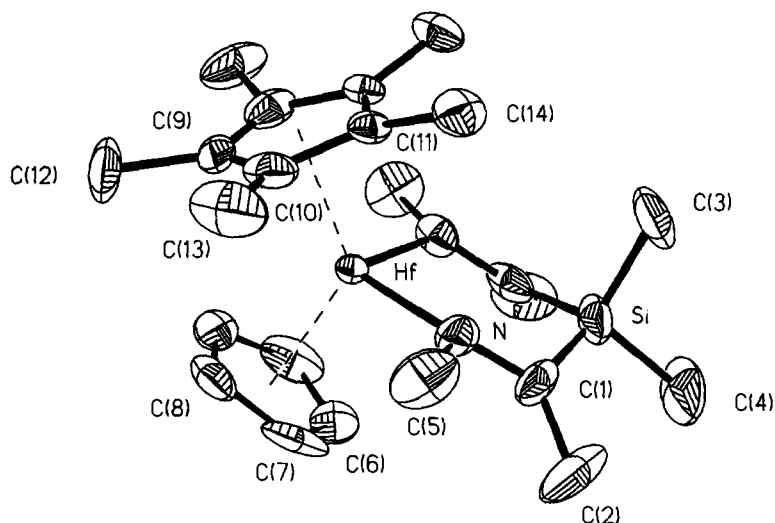


Fig. 1. Perspective view of the molecular structure of **3** with the atom numbering scheme. The thermal ellipsoids are scaled to enclose 30% probability.

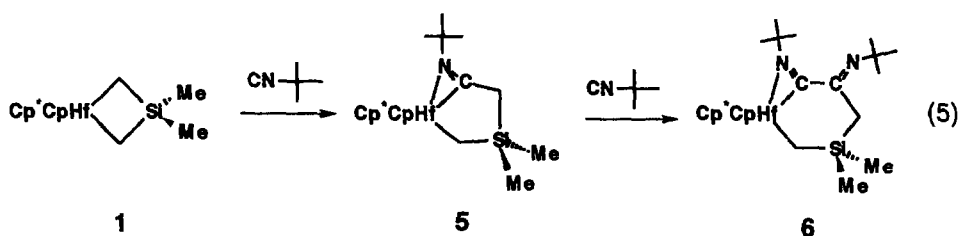
$\text{Cp}^*(c)\text{—Hf—Cp}(c)$ and $\text{N}'\text{—Hf—N}$ angles of 129.3 and $97.5(4)^\circ$, respectively, fall within the expected ranges observed for these parameters in d^0 Cp_2HfL_2 -type complexes.¹⁸

The most notable structural feature of **3** is the puckered $\text{HfN}_2\text{C}_2\text{Si}$ ring. This six-membered ring adopts a chair conformation with the folding along the $\text{N}\cdots\text{N}'$ vector being 19.3° out of the N' , Hf, N plane toward the smaller Cp ligand and the folding along the $\text{C}(1)\cdots\text{C}(1)'$ vector being 43.3° in the opposite direction toward the Cp^* ligand. Although the sums of the bond angles around $\text{C}(1)$ of 359.8° and around N of 354.4° are compatible with sp^2 hybridization at these atoms, the non-planarity of the 1-sila-3,5-diaza-4-hafnacyclohexane ring results in a $\text{C}(5)\text{—N—C}(1)\text{—C}(2)$ torsional angle of 13.2° . The puckered structure of the $\text{HfN}_2\text{C}_2\text{Si}$ ring differs significantly from the nearly planar structure observed for the six-membered $\text{ZrO}_2\text{C}_2\text{Si}$ ring of the related cyclic dienolate complex, $\text{Cp}_2^*\text{Zr}(\text{OC}(\text{=CH}_2)\text{SiMe}_2(\text{CH}_2\text{=})\text{CO})$.^{2a} In the latter case, the in-plane O p_π orbitals are able to donate to the laterally-directed LUMO of the Zr atom.¹⁹ This π -interaction introduces multiple bond character in the two Zr—O bonds, as reflected by the observed Zr—O bond distances of $1.990(2)$ and $1.987(2)$ Å. In contrast, for **3**, the p_π orbitals containing the N lone pairs are directed orthogonal to the N' , Hf, N plane, thereby minimizing their ability to donate to the corresponding LUMO at Hf. The Hf—N distance of $2.103(6)$ Å in **3** is longer than the typical Hf—N bond of $2.03\text{—}2.04$ Å in Hf dialkylamido complexes^{20,21} but is more similar to the Hf—N distance of $2.072(4)$ Å

in $\text{Cp}_2\text{Hf}(\text{N}(\text{CMe}_3)\text{C}(\text{=C}=\text{NCMe}_3)\text{C}(\text{=NCMe}_3)\text{CH}_2\text{SiMe}_2\text{CH}_2)$.²² On the other hand, it is noticeably shorter than the Hf—N bond of $2.182(12)$ Å associated with the vinylamido ligands of $\text{Cp}_2\text{Hf}(\text{N}(2,6\text{-xylyl})\text{CH}=\text{CH}\text{-py-6-Me})_2$ in which $p_\pi(\text{N}) \rightarrow d_\pi(\text{Hf})$ bonding appears to be minimal.²³

tert-Butyl isocyanide insertion chemistry of $\text{Cp}^\text{CpHf}(\text{CH}_2\text{SiMe}_2\text{CH}_2)$*

To investigate the effect of the replacement of the methyl group of CNMe with a significantly larger alkyl substituent on the isocyanide insertion chemistry, the corresponding reaction of CN-*t*-Bu with **1** was performed. Previous studies performed by Berg and Petersen have revealed that the additional steric bulk of the alkyl substituent could modify the 1,2-silyl shift pathway by either the prevention of its occurrence^{3a} or by the introduction of a dynamic equilibrium between the η^2 -iminoacyl intermediate and the corresponding cyclic enamide.⁶ The reaction of CN-*t*-Bu with **1** was monitored initially by ^1H NMR and proceeds in a stepwise manner with the sequential formation of the η^2 -iminoacyl, $\text{Cp}^*\text{CpHf}(\text{N}(\text{CMe}_3)\text{CCH}_2\text{SiMe}_2\text{CH}_2)$, **5**, and the η^2 -iminoacyl imine, $\text{Cp}^*\text{CpHf}(\text{N}(\text{CMe}_3)\text{C}(\text{=NCMe}_3)\text{CH}_2\text{SiMe}_2\text{CH}_2)$, **6** (eq. 5). The absence of any ^1H NMR resonances characteristic of an exocyclic methylene indicates that this double isocyanide insertion reaction is not accompanied by the competitive formation of a cyclic enamide. The ^1H NMR spectra of these η^2 -iminoacyl compounds



contain the appropriate number of singlets for the Cp ring protons, the methyl protons of the *tert*-Butyl substituent(s), and the protons of the two inequivalent methyl substituents of the $SiMe_2$ group. For these compounds, the two sets of methylene protons are also diastereotopic and therefore appear as AB-quartets. The ^{13}C NMR spectra of **5** and **6** contain a singlet at δ 242.9 and 239.3, respectively, which corresponds to the quaternary carbon of the η^2 -iminoacyl moiety. The ^{13}C NMR assignments are based on the comparison of the chemical shifts and $^1J_C-H$ values known for related η^2 -iminoacyl systems.^{3a,6}

Berg and Petersen previously showed that the heating of $Cp_2M(N(CMe_3)C-C(=N)CMe_3)CH_2SiMe_2CH_2$ initiated an intramolecular rearrangement that resulted in the formation of the bicyclic enediamido compound, $Cp_2M(N(CMe_3)C(CH_2SiMe_2CH_2)=CN(CMe_3))$ ($M=Zr$,^{3a} Hf⁶). Attempts to induce the analogous rearrangement for **6** were unsuccessful and eventually led to sample decomposition at temperatures above 150°C.

Description of the molecular structure of $Cp^*CpHf(N(CMe_3)C-C(=N)CMe_3)CH_2SiMe_2CH_2$

Evidence of the stereochemical influence of the Cp^* ligand on the second insertion step leading to the formation of **6** is provided by the results of an X-ray structural analysis. A perspective view of its molecular configuration is displayed in Fig. 2 with the non-hydrogen atom labeling scheme. The hafnium atom is located in a chiral pseudotetrahedral ligand environment consisting of a π -bonded pentamethylcyclopentadienyl ring, a π -bonded cyclopentadienyl ring, an η^2 -iminoacyl moiety, and a σ -bonded methylene group. The compound crystallizes in the non-centrosymmetric space group $Pna2_1$ as a racemic mixture. The η^2 -iminoacyl group adopts the expected "N-outside" configuration with the η^2 -iminoacyl carbon, C(1), forming a single C—C bond with the imine carbon, C(2). The Hf—N(1) and Hf—C(1) bond distances of

2.242(8) and 2.201(12) Å, respectively, are *ca* 0.02 Å longer than the corresponding bond distances in $Cp_2Hf(N(CMe_3)C-C(=N)CMe_3)CH_2SiMe_2CH_2$.⁶ These slightly longer distances probably reflect the more crowded metal coordination environment due to the presence of the larger Cp^* ligand. This apparent weakening in the η^2 -iminoacyl interaction, however, is compensated by a noticeably shorter Hf—C(4) bond of 2.28(2) Å, which is *ca* 0.065 Å less than the Hf—C(methylene) bond in $Cp_2Hf(N(CMe_3)C-C(=N)CMe_3)CH_2SiMe_2CH_2$.⁶

Although the atom connectivity within the two adjacent metallacyclic rings of **6** is analogous to that of $Cp_2Hf(N(CMe_3)C-C(=N)CMe_3)CH_2SiMe_2CH_2$, the replacement of a Cp ring in the latter with the sterically more demanding Cp^* ligand alters the conformational structure associated with the six-membered hafnacyclic ring and significantly changes the relative orientation of the exocyclic imine functionality. The molecular structures of these two η^2 -iminoacyl imine complexes are shown side-by-side in Fig. 3 looking down the C(1)—C(2) bond. The observed structural differences can be understood by considering the stereochemical influence of the Cp^* ligand on the second isocyanide insertion step that results in the formation of the C(1)—C(2) bond. NMR tube experiments clearly indicate that this double insertion reaction occurs in a stepwise manner, with **5** being converted cleanly to **6**. Isotopic labeling experiments performed on a related Zr system have shown^{2b} that the second insertion step proceeds with displacement rather than retention of the original η^2 -iminoacyl moiety of $Cp_2Zr(N(CMe_3)C(CH_2SiMe_2CH_2))$. Non-parameterized Fenske-Hall Hartree-Fock SCF MO calculations⁸ have shown that the LUMO of $Cp_2Zr(N(CMe_3)C(CH_2SiMe_2CH_2))$ is comprised of the iminoacyl π_{C^*N} orbital which is stabilized by interaction of the iminoacyl C p_z orbital with the Zr $4d_{xz}$ orbital. Because the plane of the three-membered MCN ring of these η^2 -iminoacyl complexes bisects the

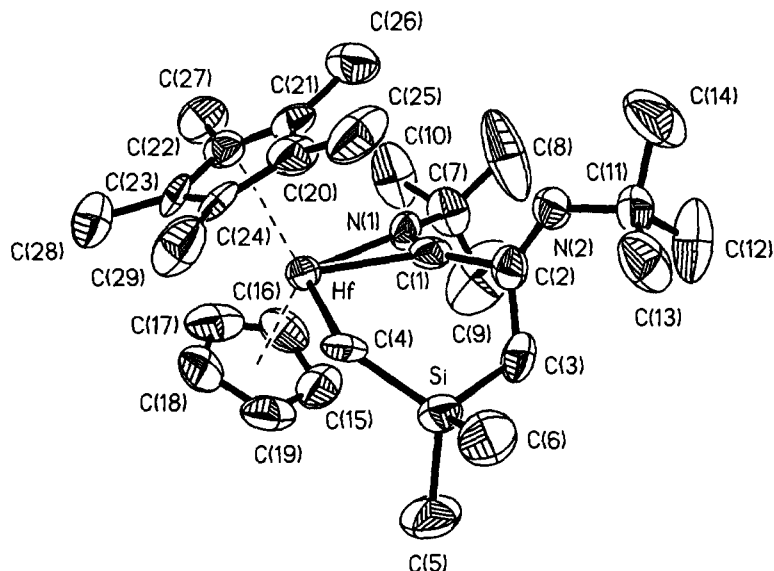


Fig. 2. Perspective view of the molecular structure of **6** with the atom numbering scheme. The thermal ellipsoids are scaled to enclose 50% probability.

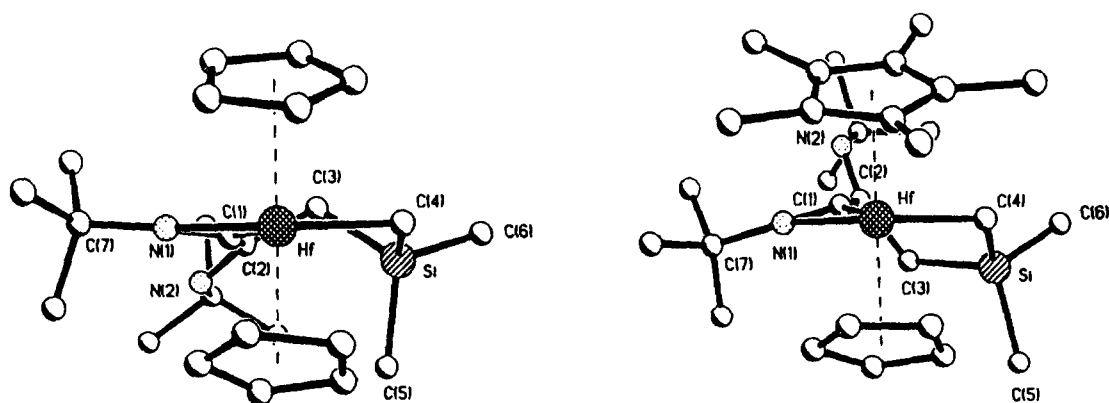


Fig. 3. Comparison of the relative orientations of the exocyclic imine functionality in $\text{Cp}_2\text{Hf}(\text{N}(\text{CMe}_3)\text{C}-\text{C}(=\text{NMe}_3)\text{CH}_2\text{SiMe}_2\text{CH}_2)$ (left) and **6** (right) as viewed down the $\text{C}(1)-\text{C}(2)$ bond vector.

metallocene wedge, an incoming nucleophilic substrate can approach the LUMO from either side of this plane. For $\text{Cp}_2\text{Hf}(\text{N}(\text{CMe}_3)\text{CCH}_2\text{SiMe}_2\text{CH}_2)$ the probability of the isocyanide attacking the electrophilic η^2 -iminoacyl carbon from either side of the HfCN plane should be the same. In contrast, the bulky Cp^* ligand of **5** lies partially over one face of the HfCN ring, thereby blocking CN-*t*-Bu from approaching the side facing the Cp^* ligand. As a result, CN-*t*-Bu preferentially attacks from the opposite side. The subsequent displacement of the η^2 -iminoacyl group by the coordinated isocyanide directs this group away from the metal, eventually placing the resultant imine group on the same side as the Cp^* ligand in

6. This arrangement produces a rather large $\text{N}(1)-\text{C}(1)-\text{C}(2)-\text{N}(2)$ torsional angle²⁴ of $(-)$ 78.0°, which is significantly different from the corresponding torsional angle of $(+)$ 38.9° in $\text{Cp}_2\text{Hf}(\text{N}(\text{CMe}_3)\text{C}-\text{C}(=\text{NMe}_3)\text{CH}_2\text{SiMe}_2\text{CH}_2)$. The large (negative) dihedral angle also leads to an alteration in the puckering of the six-membered hafnacyclic ring with C(3) now positioned well below the Hf, N(1), C(4) plane that bisects the metallocene wedge and produces an 0.07 Å increase in the displacement of C(1) out of the Hf, N(1), C(2) plane. Because only one of the two possible diastereomers (which differ in terms of the relative orientation of the Cp^* ligand and imine functionality) is observed, the introduction of the Cp^*

ligand clearly has a substantial stereochemical influence on the insertion of the second equivalent of CN-*t*-Bu.

The steric size of the Cp* ligand in **6** may also account for the inability of **6** to rearrange intramolecularly upon heating to the corresponding bicyclic enediamidate complex. Although the relative disposition of the exocyclic imine N atoms of **6** and of $Cp_2Hf(N(CMe_3)C-C(=NCMe_3)CH_2SiMe_2CH_2)$ shows that the imine N of **6** should travel a shorter effective distance to complete the chelation of the enediamido ligand, steric interactions between the methyl groups of the Cp* ligand and *tert*-Butyl substituent could impede the path of the imine N to the Hf. However, other factors such as the relative differences in the strengths of the Hf—C(methylene) bonds and the conformational structures of the six-membered hafnacyclic rings of **6** and $Cp_2Hf(N(CMe_3)C-C(=NCMe_3)CH_2SiMe_2CH_2)$ may also affect the amplitude of the activation barrier associated with this intramolecular rearrangement and therefore cannot be overlooked.

CONCLUDING REMARKS

The presence of the Cp* ligand in **1** has provided an opportunity to evaluate its stereochemical influence on the competitive reductive coupling and 1,2-silyl shift reactions associated with the multiple insertion of CNMe and CN-*t*-Bu into the Hf—C bond(s) of the electrophilic 1-sila-3-hafnacyclobutane ring. Whereas the insertion reactions of **1** with CNMe are consistent with our previous observations,⁶ the corresponding reaction of **1** with CN-*t*-Bu indicates that the steric size of the Cp* ligand can control the diastereoselectivity of the C—C bond forming reaction associated with the reductive coupling pathway. The steric bulk of the Cp* directs the nucleophilic attack of CN-*t*-Bu at the η^2 -iminoacyl carbon of **5** to the side opposite from the Cp* ligand, thereby resulting in the formation of a single η^2 -iminoacyl imine diastereomer, **6**.

Acknowledgments—Financial support for this research was provided by the National Science Foundation (CHE-9113097). We also wish to acknowledge the financial support provided by the Chemical Instrumentation Program of the National Science Foundation (Grant No. CHE-9120098) for the acquisition of a Siemens P4 X-ray diffractometer in the Department of Chemistry at West Virginia University.

Supplementary material available—Tables of crystallo-

graphic data (9 pages) from the crystallographic analyses of **3** and **6**.

REFERENCES

1. This work is based in part on the Diplomthesis submitted by Lioba Kloppenburg to the University of Münster in January, 1994.
2. J. L. Petersen and J. W. Egan Jr, *Organometallics* 1987, **6**, 2007.
3. (a) F. J. Berg and J. L. Petersen, *Organometallics* 1989, **8**, 2861; (b) F. J. Berg and J. L. Petersen, *Organometallics* 1991, **10**, 1599; (c) F. J. Berg and J. L. Petersen, *Tetrahedron* 1992, **48**, 4749.
4. Leading references for the intramolecular 1,2-silyl shift rearrangement include: (a) D. C. Sonnenberger, E. A. Mintz and T. J. Marks, *J. Am. Chem. Soc.* 1984, **106**, 3484; (b) M. F. Lappert, C. L. Raston, L. M. Engelhardt and H. A. White, *J. Chem. Soc., Chem. Commun.* 1985, 521; (c) R. P. Phanalp and R. A. Andersen, *Organometallics* 1983, **2**, 1675; (d) A. Dormond, A. A. E. Bouadili and C. Moise, *J. Chem. Soc., Chem. Commun.* 1985, 914.
5. Leading references for the reductive coupling of CO and isocyanides by electrophilic organometallic reagents include: (a) D. M. Roddick and J. E. Bercaw, *Chem. Ber.* 1989, **122**, 1579; (b) K. G. Moloy, P. J. Fajan, J. M. Manriquez and T. J. Marks, *J. Am. Chem. Soc.* 1986, **108**, 56; (c) G. Erker, *Angew. Chem., Int. Ed. Engl.* 1989, **28**, 397; (d) C. C. Cummins, G. D. Van Duyne, C. P. Schaller and P. T. Wolczanski, *Organometallics* 1991, **10**, 164; (e) W. J. Evans, *Adv. Organometal. Chem.* 1985, **24**, 131; (f) B. K. Campion, R. H. Heyn and T. D. Tilley, *Organometallics* 1993, **12**, 2584; (g) L. D. Durfee, A. K. McMullen and I. P. Rothwell, *J. Am. Chem. Soc.* 1988, **110**, 1463; (h) J. R. Bocarsly, C. Floriani, A. Chiesa-Villa and C. Guastini, *Organometallics* 1986, **5**, 2380; (i) B. Hessen, J. Blenkins, J. Teuben, G. Helgesson and S. Jagner, *Organometallics* 1989, **8**, 830.
6. F. J. Berg and J. L. Petersen, *Organometallics* 1993, **12**, 3890.
7. C. Valero, M. Grehl, D. Wingbermhühle, L. Kloppenburg, D. Carpenetti, G. Erker and J. L. Petersen, *Organometallics* 1994, **13**, 415.
8. The topology and orbital composition of this LUMO is analogous to the carbenium-type representation described originally by Hoffmann and co-workers⁹ for electrophilic metallocene η^2 -acyl complexes.
9. K. Tatsumi, A. Nakamura, P. Hofmann, P. Stauffert and R. Hoffmann, *J. Am. Chem. Soc.* 1985, **107**, 4440.
10. D. G. Sekutowski and G. D. Stucky, *Inorg. Chem.* 1975, **14**, 2192.
11. R. E. Shuster, J. E. Scott and J. Casanova Jr, *Org. Synth.* 1973, **5**, 773.
12. R. S. Threlkel, J. E. Bercaw, P. F. Seidler and R. G. Bergman, *Org. Synth.* 1987, **65**, 42.

13. W. R. Tikkanen, J. Z. Liu, J. W. Egan Jr and J. L. Petersen, *Organometallics* 1984, **3**, 825.
14. P. T. Wolczanski and J. E. Bercaw, *Organometallics* 1982, **1**, 798.
15. D. M. Roddick, M. D. Fryzuk, P. F. Seidler, G. L. Hillhouse and J. E. Bercaw, *Organometallics* 1985, **4**, 97.
16. SHELXL-93 is a FORTRAN-77 program (Professor G. Sheldrick, Institut für Anorganische Chemie, University of Göttingen, D-37077 Göttingen, Germany) for single crystal X-ray structural analyses.
17. The values of these discrepancy indices were calculated from the expressions $R_1 = \Sigma |F_o| - |F_c| / \Sigma |F_o|$ and $wR_2 = [\Sigma (w_i(F_o^2 - F_c^2)^2) / \Sigma (w_i F_o^2)]^{1/2}$ and the standard deviation of an observation of unit weight (GOF) is equal to $[\Sigma (w_i(F_o^2 - F_c^2)^2) / (n - p)]^{1/2}$, where n is the number of reflections and p is the number of parameters varied during the last refinement cycle.
18. (a) W. E. Hunter, D. C. Hrnecir, R. V. Bynum, R. A. Pentilla and J. E. Atwood, *Organometallics* 1983, **2**, 750; (b) C. Krüger, G. Müller, G. Erker, U. Dorf and K. Engel, *Organometallics* 1985, **4**, 215; (c) G. Erker, U. Korek and J. L. Petersen, *J. Organometal. Chem.* 1988, **355**, 121; (d) P. G. Gassman and C. H. Winter, *Organometallics* 1991, **10**, 1592; (e) H.-G. Woo, R. H. Heyn and T. D. Tilley, *J. Am. Chem. Soc.* 1992, **114**, 5698.
19. J. Lauher and R. Hoffman, *J. Am. Chem. Soc.* 1976, **98**, 1729.
20. (a) C. Airoidi, D. C. Bradley, H. Chudzynska, M. B. Hursthouse, K. M. Abdul Malik and P. R. Raithby, *J. Chem. Soc., Dalton Trans.* 1980, 2010; (b) G. L. Hillhouse, A. R. Bulls, B. D. Santasiero and J. E. Bercaw, *Organometallics* 1988, **7**, 1309.
21. Although Bercaw and co-workers^{20b} suggest that the Hf—N distance of 2.027(8) Å in Cp₂Hf(H)(NHMe) represents a reasonable value for a Hf=N(sp²) bond distance, they estimated from variable temperature NMR measurements that the activation barrier for oscillation about the Hf—N bond in this complex is less than 10 kcal mol⁻¹, which places an upper limit on the magnitude of the Hf—N π-interaction for a simple hafnocene amido complex.
22. The structure of Cp₂Hf(N(CMe₃)C(=C=NCMe₃)C(=NCMe₃)CH₂SiMe₂CH₂) is isomorphous to that of the Zr analogue.⁷
23. S. M. Beshouri, P. E. Fanwick, I. P. Rothwell and J. C. Huffman, *Organometallics* 1987, **6**, 891.
24. A positive torsional angle indicates that the C(1)—N(1) bond vector must be rotated counter-clockwise in order for its projection to superimpose on the C(2)—N(2) bond vector.